Available online at www.sciencedirect.com
ScienceDirect
Applied Surface Science 253 (2007) 4641–4648
applied surface science
www.elsevier.com/locate/apsusc

Investigation of chemisorbed oxygen, surface segregation and effect of post-treatments on $La_{0.8}Sr_{0.2}MnO_3$ powder and screen-printed layers for solid oxide fuel cell cathodes

N. Caillol [a], M. Pijolat [a,*], E. Siebert [b]

[a] LPMG CNRS UMR 4158, Centre SPIN, Ecole Nationale Supérieure des Mines de Saint-Etienne, 158 cours Fauriel, 42023 Saint Etienne, France
[b] LEPMI CNRS UMR 5631, Institut National Polytechnique de Grenoble, 1130, rue de la Piscine, 38402 Saint Martin d'Hères, France

Received 20 September 2006; received in revised form 9 October 2006; accepted 9 October 2006
Available online 29 November 2006

Abstract

In order to better understand the mechanism of the reaction of oxygen reduction at the surface of strontium doped lanthanum manganites (LSM) cathodes in solid electrolyte fuel cells (SOFC), the surface properties of $La_{0.8}Sr_{0.2}MnO_3$ powders and screen-printed layers have been characterised by various techniques.

Strontium enrichment at the surface has been evidenced by X-ray photoelectron spectroscopy according to the conditions of annealing (temperature, oxygen pressure) and polarisation treatments of the samples.

The interaction between oxygen and $La_{0.8}Sr_{0.2}MnO_3$ for SOFC cathodes has been studied by thermo-programmed desorption, in situ infrared spectrometry and calorimetry. The results indicate that various adsorbed oxygen species may exist on the surface of LSM depending on temperature.

The presence of various adsorbed oxygen species and the surface Sr segregation are important factors to consider in the mechanism of oxygen reduction at LSM SOFC cathodes since they could be responsible for many discrepancies between the interpretations that can be found in the literature data.

PACS : 82.47.−a

Keywords: LSM; SOFC; Adsorbed oxygen species; Screen-printing; Segregation

1. Introduction

Perovskite-type oxide $La_{0.8}Sr_{0.2}MnO_3$ (LSM) is the standard material used for cathodes in solid oxide fuel cells (SOFC). Although this compound does not achieve the best performances, it represents, combined with YSZ for electrolyte, an interesting compromise for an optimal performance of the device. Furthermore, since LSM has been the subject of many previous studies, numerous data on microstructural and electrochemical characterisations have been reported [1,2]. It appears that a large number of parameters have a significant importance for optimising the reaction of oxygen reduction that takes place at LSM cathodes.

Due to the very low ionic conductivity of LSM phases, the oxygen reduction is thought to be located at the triple phase boundary (TPB) between cathode, electrolyte and gas. Oxygen adsorption and its transport towards the electrolyte are steps generally involved in the mechanisms of the literature [3–14]. In Table 1 are summarised the possible mechanisms and their corresponding elementary steps encountered in the literature. Two kinds of mechanisms have been proposed: surface- and bulk-type. Many authors have interpreted their data (in general from impedance spectrometry which is the technique used for electrochemical characterisations and kinetics analysis) by means of surface-type mechanisms, due to the improbable transport of oxygen via bulk oxygen vacancies. It can be seen from Table 1 that many possibilities have been proposed for the

* Corresponding author. Tel.: +33 4 77 42 01 52; fax: +33 4 77 49 96 94.
E-mail address: mpijolat@emse.fr (M. Pijolat).

0169-4332/$ – see front matter © 2006 Elsevier B.V. All rights reserved.
doi:10.1016/j.apsusc.2006.10.019

Table 1
Limiting steps of the cathodic reaction encountered in literature

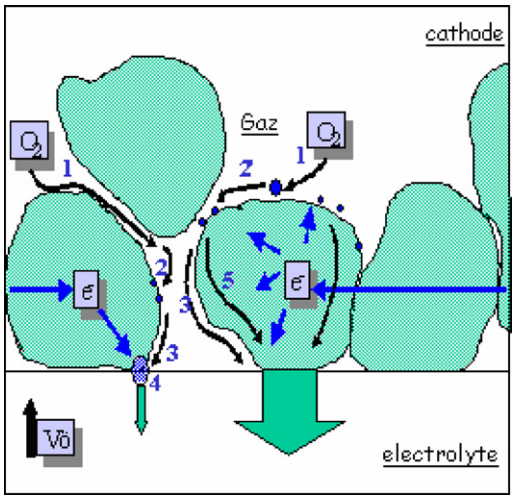

Mechanism	Limiting step	Reference
Surface	Gas diffusion (**1**)	[3]
	Dissociative adsorption (**2**)	[4–6]
	Dissociation alone (**2′**)	[7,8]
	Surface diffusion (**3**)	[9,3]
	Charge transfer (**4**)	[10]
	Mixed regime	
	Diffusion/transfer	[11]
	Dissociation/transfer	[12], etc.
Bulk	Bulk diffusion (**5**)	
	Porous layer	[13]
	Dense layer	[14]

rate-limiting step of the oxygen reduction. Despite the numerous attempts to understand the kinetics of such a simple reaction, no real consensus has yet been reached. Considering the numerous parameters and effects that may have an influence on the kinetics, this is not surprising. From a detailed analysis of the published results, it appears that most of the discrepancies between laboratories may be explained by three main considerations:

- the surface composition, as emphasised by Mogensen et al. [15]: impurities and other segregation effects at the reaction zone have probably a major impact over the reaction;
- the microstructure: it differs greatly from one elaboration technique to the other;
- the evaluation of the electrochemical properties: the difficulties linked to the interpretation of impedance spectra must not be neglected.

Moreover, the lack of knowledge on the chemisorbed oxygen species resulting from the interaction between oxygen and LSM surfaces has to be underlined.

Following this quick analysis of the situation, it appears essential to have a control over the properties of the device under study by mastering precisely all the elaboration steps of the electrodes before testing. However, this should be completed by improvement of the knowledge of the surface properties of the material under study, considering both the oxygen chemisorbed species and the possible effects of surface enrichment according to the various treatments of the cathode, i.e. temperature, gaseous atmosphere and polarisation in electrochemical cells.

In the present study, we concentrate on the surface properties of $La_{0.8}Sr_{0.2}MnO_3$ in powders and in screen-printed thick layers: surface segregation, effect of post-treatments (annealing and polarisation) on the surface segregation, and characterisation of oxygen chemisorbed species.

Screen-printing is a very convenient technique for the electrodes' fabrication as it is interesting at an industrial scale for producing low cost, reproducible and stable thick layers. Their microstructure has been characterised by scanning electron microscopy (SEM), mercury porosimetry, and BET (krypton) specific surface area.

To determine segregation effects, the surface of samples (as-prepared or after various post-treatments) have been analysed by X-Ray photoelectron spectroscopy (XPS). To learn about the chemisorbed oxygen species, the techniques used have been thermo-programmed desorption (TPD), in situ Fourier-transformed infrared spectrometry, and calorimetry.

2. Experimental

2.1. Samples: powders and screen-printed layers

The starting powder was a commercial LSM powder ($La_{0.8}Sr_{0.2}MnO_3$) purchased from Superconductive (''initial powder''). A thermal treatment of this powder was performed at 1000 °C during 2 h in air (''1000 °C powder'').

The inks for screen-printing deposition were prepared with the initial powder mixed to an organic binder from ESL (V400-A) and solvent (400 thinner) with 50 wt.% of powder. The inks are directly deposited on either dense sintered YSZ pellets or alumina substrates using a semi-automatic AUREL C890 screen-printer, and a 180-mesh mask. In order to reach a desired electrode thickness, between one to five layers are piled up. Between each deposition, the layers are dried at 100 °C. The electrode is then sintered at 1200 °C for 2 h with a 15 °C min^{-1} heating rate under ambient air. A single deposited layer is approximately 20 μm thick and five deposits lead to a 65 μm thick layer.

2.2. Characterisation techniques

The microstructure of both powder and LSM layers was carefully characterised using conventional structural and textural techniques: scanning electron microscopy (SEM), JEOL JSM6400, specific surface area measurements (BET) to quantify the surface accessible to the gas phase (Micromeritics, Asap 2000, krypton), Hg-porosimetry to quantify porosity and to obtain the pore size distribution (Micromeritics, AutoporeV). For all these characterisations, and for practical reasons, the screen-printed layers are deposited on commercial aluminate substrates instead of YSZ pellets.

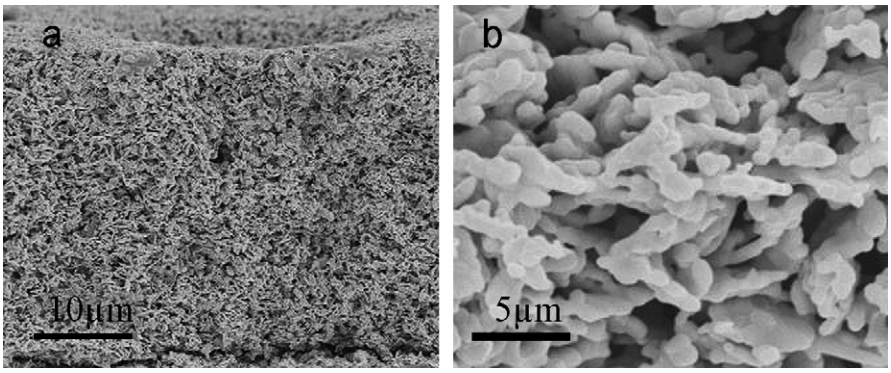

Fig. 1. (a) SEM pictures of the cross section of LSM screen-printed layer, five deposits on an alumina plate; (b) close up on the microstructure within the layer.

Surface composition was analysed by means of XPS using a Cameca spectrometer equipped with a X-radiation source of Mg Kα (450 W), a MAC 3 analyser and a single channeltron. For these analyses, powder samples were pressed on indium sheets.

In order to characterise chemisorbed oxygen on LSM powder, thermo-programmed desorption experiments (TPD) were carried out. For these experiments, 0.1 g of powder is placed in a tube where secondary vacuum is made. After heating up to 900 °C so as to desorb all adsorbed species at the surface, the powder is put in contact with 50 hPa of oxygen for a given time, t, at a given temperature, T_A. Vacuum is once more made for 20 min prior to recording by mass spectrometry ($m/e = 32$) the oxygen species desorbing from the powder while heating from T_A up to 900 °C at 20 °C min^{-1}. After subtraction of a background spectra obtained from a non-oxygen pre-treated experiment, these thermograms allow us to distinguish different adsorbed species from their temperatures of desorption, each adsorbed species being characterised by a peak which intensity is proportional to the rate of desorption.

In situ infrared spectra were recorded using diffuse reflectance Fourier transformed infrared spectrometry (DRIFTS) cell mounted on a Biorad FTS 185 spectrometer. The sample (≈1% LSM in KBr) was placed in a Spectra tech cell (0030-13) which permits operation in controlled gaseous atmosphere up to 600 °C. The adsorptions were performed on samples first treated at 600 °C in helium during 20 min to remove eventual contamination of the surface. Then the spectra were recorded at the desired temperature under helium or oxygen/helium (50/50) (Alphagaz 1 from Air liquide). The background spectra obtained with pure KBr in the same gas and temperature conditions were systematically subtracted to the spectra recorded with LSM in KBr.

Calorimetry tests were performed using a Setaram Tian and Calvet calorimeter, on 0.19 g of LSM pellets previously annealed at 1200 °C during 2 h. The calorimeter was first evacuated up to ≈1 hPa, and then oxygen was introduced up to a pressure of 200 hPa. After stabilisation of the calorimeter signal, the vacuum was made back to 1 hPa. Various adsorption/desorption cycles have been performed at 700, 750, 800, 830 and 850 °C.

3. Results and discussion

3.1. Powder and screen-printed layer microstructure

The specific surface areas of the initial and 1000 °C powders are equal to 4 and 1 $m^2\ g^{-1}$, respectively. The corresponding values of the mean diameter, which can be deduced assuming a spherical shape of the particles, are 0.24 µm for the initial powder and 1 µm for the 1000 °C powder. Specific surface areas measured on screen-printed layers were found to be equal to 1 $m^2\ g^{-1}$.

Presented in Fig. 1 are the typical SEM views of the cross sections of screen-printed layers of initial powder cathodes. Fig. 1a shows it to be homogeneous and uniform over the whole section. There is in particular no clearly visible separation of the successively deposited layers (five layers in the case of Fig. 1a).

Fig. 2 presents the pore size distribution obtained from mercury porosimetry for the initial powder and two screen-printed layers, as-prepared and post-treated 1 week at 800 °C under dry air. It can be seen that the elaboration process of the screen-printed layers does not modify significantly the pore size distribution (great majority of 1 µm pores in both cases), only the volume of pores shrinks from 1.16 for the powder to 0.3 mL/g for the layer. After aging at 800 °C during a week, the

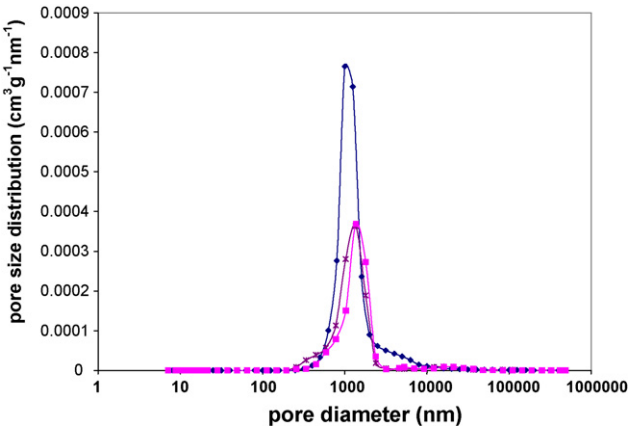

Fig. 2. Typical pore size distributions of screen-printed layers sintered at 1200 °C for 2 h compared to the initial commercial powder: (◆) initial powder; (*) screen-printed layer; (■) layer post-treated 1 week at 800 °C.

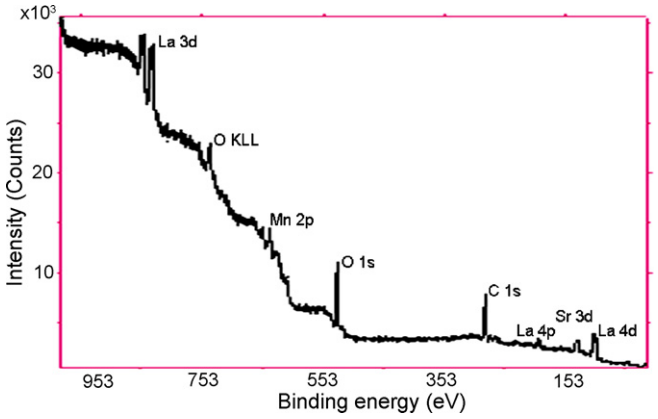

Fig. 3. Mg Kα-excited XPS spectrum for $La_{0.8}Sr_{0.2}MnO_3$.

microstructure of the layers does not change. No significant change of specific area was measured and only a slight increase in pore diameter is visible.

From the total pore volume, knowing the dimensions and weight of the layer, its porosity can be calculated; its value is found to be equal to 60%, which is in good agreement with the value deduced from a model of dense packed spheres:

$$d_{\text{pore}} = \frac{2}{3}\frac{\varepsilon}{1-\varepsilon}d_{\text{grain}} \quad (1)$$

where d_{pore} is the pore diameter (=1 μm), d_{grain} the grain diameter (=1 μm) and ε is the porosity of the layer.

From these results, it can be deduced that the process of elaboration of the LSM screen-printed layers does not modify significantly the morphological properties of the LSM particles. Characterisations can therefore be performed either on powder or on layers, indifferently; only post-treatments will be responsible for eventual significant surface modifications. In particular, the good thermal stability of the layer microstructure allows measurements at high temperature without any risk of damaging the LSM layer.

3.2. Surface segregation

Fig. 3 shows the XPS spectrum obtained with the initial LSM powder. A carbon contamination was detected in all samples since they have been analysed without any preparation treatment. Using the effective cross sections of elements [16], it is possible to determine the stoichiometric ratios among La, Sr, Mn and O from the intensity ratios. The intensities of the peaks La $3d_{5/2}$, La $3d_{3/2}$, La $4p_{(3/2+1/2)}$, La $4d_{(5/2+3/2)}$, Sr 3d, Mn $2p_{3/2}$, Mn $2p_{1/2}$ and O 1s have been taken after background correction. The mean average value of the ratios obtained using the various possible combinations among all the peaks were determined for La/Mn, La/Sr and La/O stoichiometries. Table 2 reports the values of the stoichiometric ratios for the initial powder, the 1000 °C powder, and screen-printed layers as-prepared and post-treated at 800 °C for 1 week. Expected ratios corresponding to $La_{0.8}Sr_{0.2}MnO_3$ are given in the second column of Table 2. The errors indicated in the table have been evaluated by calculating the standard deviation of the ratios obtained using the different peaks of each element.

The La/Sr ratios obtained for the initial and 1000 °C powders are identical to that expected from LSM stoichiometry. Both samples however exhibit Mn deficiency. The La/O ratio is always lower than expected, but this can be due to oxygen containing contamination-species, so the slight changes observed from a sample to another will not be taken into consideration.

The results obtained with the screen-printed LSM layers show Sr enrichment for the as-prepared layer that disappears after annealing at 800 °C. This reveals that Sr migration is favoured by the 1200 °C treatment during the elaboration process. The fact that strontium segregates at the surface of LSM after elaboration has been reported previously [17–21]. But it is interesting to observe that this segregation disappears when the electrode is left at 800 °C, which means that when electrochemical tests are performed at equilibrium under air at temperatures up to 800 °C, the surface of LSM particles recovers the expected stoichiometry.

The impact of the oxygen pressure over this segregation has also been looked at due to a comparison between samples treated at 900 °C (in two distinct O_2/N_2 atmospheres: ''rich'' (20/80) and ''poor'' (1/99). The results shown in Table 3 indicate that Sr segregation is favoured by the oxygen ''poor'' atmosphere since La/Sr is as low as 2.6 instead of 4.2 for the oxygen ''rich'' atmosphere. This is in agreement with a recent work on $La_{0.5}Sr_{0.5}MnO_3$ [20].

Table 3
La/Sr stoichiometric ratios depending on pressure and polarisation treatments

Cell	La/Sr
Pressure	
Low oxygen pressure	2.6 ± 0.4
High oxygen pressure	4.2 ± 0.4
Polarisation	
Reference	2.9 ± 0.5
Cathodic side	2.6 ± 0.3
Anodic side	3.2 ± 0.1

Table 2
Stoichiometric ratios between the elements

Ratio	Expected	Initial powder	1000 °C powder	As-prepared screen-printed layer	Screen-printed layer after 800 °C under air (1 week)
N_{La}/N_{Mn}	0.8	1.3 ± 0.3	1.3 ± 0.3	1.7 ± 0.4	1.9 ± 0.6
N_{La}/N_{Sr}	4	4.0 ± 0.5	4.1 ± 0.2	2.4 ± 0.5	4.2 ± 0.4
N_{La}/N_{O}	0.27	0.22 ± 0.05	0.25 ± 0.02	0.24 ± 0.05	0.24 ± 0.03

To characterise the electrochemical properties of screen-printed LSM electrodes, a treatment under strong polarisation at 800 °C under ambient air was performed on a symmetrical electrochemical cell LSM/YSZ/LSM [2,22]. The results presented in Table 3 show that the strontium segregation increases with cathodic polarisation. In the literature, a cathodic pre-treatment is often done to increase the electrochemical performance of cathodes. This optimisation is attributed to the elimination of SrO at the surface by polarisation [18]. In the Table, the reference was a fragment of the cell that was not submitted to the polarisation treatment.

From this study we gather that the strontium segregation at the surface of LSM is function of temperature, oxygen pressure and polarisation. Hence, the interaction between oxygen and LSM surface should be dependent of the operating conditions of LSM based cathodes in SOFC devices, mainly with temperature and polarisation. Some authors have proposed that the Sr surface enrichment was due to the formation of SrO [20], the presence of which could greatly modify the mechanism of the cathodic reaction. The effects on Sr segregation of post-treatment temperature, oxygen pressure and polarisation, certainly has an important role on the differences in the mechanisms and rate-controlling steps observed in the literature (cf. Section 1).

3.3. Oxygen chemisorption

Oxygen chemisorption on LSM has been studied by means of TPD, FTIR and calorimetry. Following the previous observations concerning the strontium segregation it is worth indicating that both TPD and calorimetric analyses are carried out on LSM with strontium segregation. Indeed, in these experiments the samples have been maintained under vacuum at elevated temperature (600–900 °C) for long periods.

3.3.1. Thermo-programmed desorption

Fig. 4 shows a series of TPD thermograms obtained after adsorption of oxygen (50 hPa and 30 min exposure) at various temperatures. Up to six distinct desorption peaks can be observed according to the temperature of exposure. The existence of several desorption peaks is an indication of the existence of various kinds of oxygen species. It must be noticed that for the highest temperatures (near 900 °C) the contribution of oxygen coming from the bulk structure of LSM cannot be excluded since LSM is known to be a non-stoichiometric compound [23].

From TPD thermograms obtained after adsorption of oxygen at 600 °C (50 hPa) during various periods (Fig. 5), it is interesting to see that at least three peaks of desorption can be distinguished, at about 700, 790 and 875 °C, clearly indicating the complexity of the interactions between O_2 and LSM in this temperature and pressure range. Moreover, the kinetics of adsorption appears to be quite slow, as the intensity of the peaks was found to increase regularly with the time of exposure from 1 to 120 min.

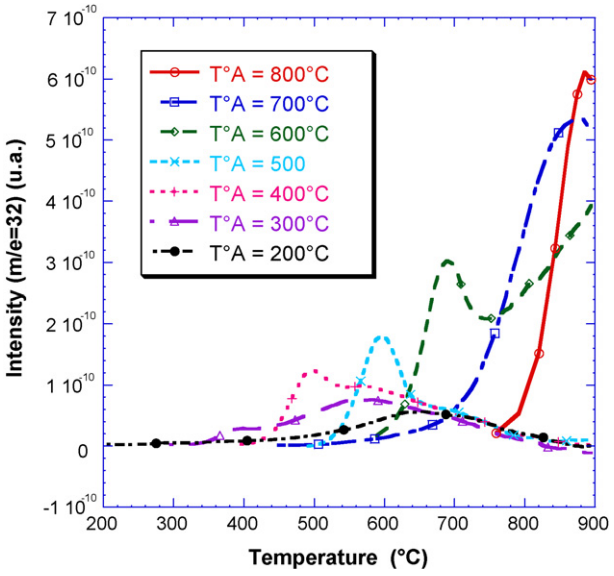

Fig. 4. TPD thermograms of the mass 32 corresponding to desorptions obtained after 30 min adsorption of 50 mbar oxygen on LSM at different temperatures (*T*, °C).

3.3.2. Infrared spectroscopy

To try to identify these oxygen species, in situ DRIFTS analyses were carried out. The spectra, presented in Fig. 6, were obtained with two conditions of gaseous atmosphere, helium and a mixture of oxygen and helium, and at various temperatures from ambient to 600 °C. They show the formation, at high temperature (500–600 °C) and in both atmospheres, of two chemisorbed species with bands at 1012–1014 and 825 cm^{-1}. These bands are located in the range of bands for oxygen species on an oxide surface [24]. Considering the literature data, they can be attributed to O_2^- and O_2^{2-} (for 1012 and 825 cm^{-1}, respectively).

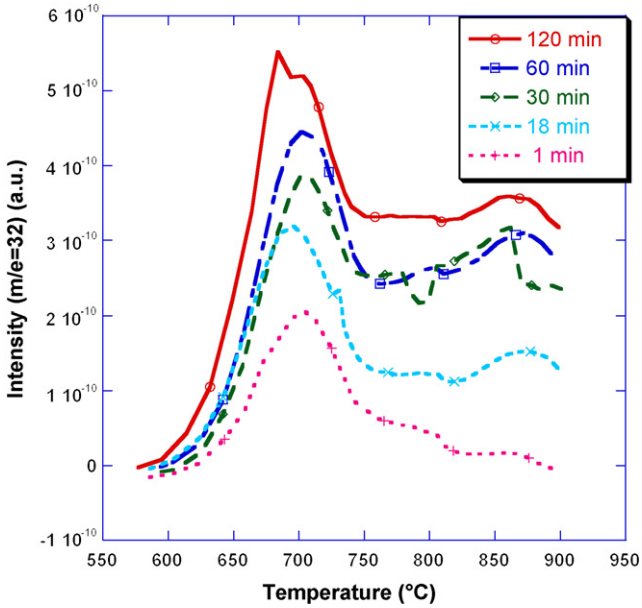

Fig. 5. Thermograms obtained after adsorption at 600 °C of 50 mbar of oxygen during 1, 18, 30, 60 and 120 min.

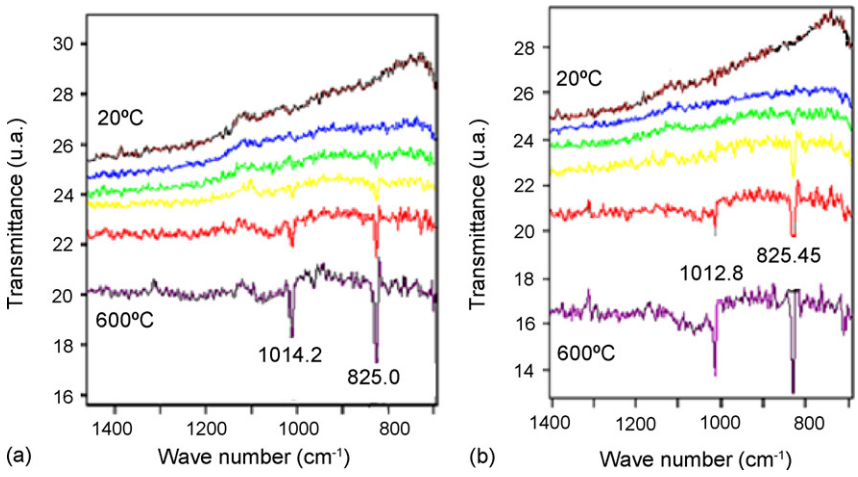

Fig. 6. DRIFT spectra, of LSM initial powder at temperatures varying from room temperature to 600 °C: (a) under helium and (b) under oxygen.

These species appear when heating the LSM powder (Fig. 6), disappear when cooling, and are present both under oxygen or helium atmospheres. This can be explained if oxygen is adsorbed in a non-ionised state at room temperature at the surface of LSM (considering the oxygen species desorbing above 600 °C observed by TPD, this is very likely) and if, when heated, these oxygen capture free electrons from LSM. Such adsorbed oxygen species are not removed during treatment under helium up to 600 °C, so the intensities of the IR bands are almost equal under helium and oxygen.

The FTIR results are in agreement with TPD experiments on the fact that distinct species of chemisorbed oxygen may be present at the surface of LSM, even simultaneously, according to temperature conditions. Elevated temperatures would favour the ionisation of these species.

3.3.3. Calorimetry

Calorimetric tests where performed on LSM screen-printed layers at different oxygen pressures and temperatures. The calorimeter records, at a constant temperature, the power released as a function of time during oxygen adsorption, as illustrated by the curves of Fig. 7 (800 °C and 200 hPa of oxygen), followed after stabilisation of the signal by its desorption. In usual adsorption experiments, the total area under the power curve corresponds to enthalpy of adsorption (or desorption when evacuating). Comparing the value obtained during the adsorption phase (14 J) and desorption (13 J) phase shows that the adsorption step is perfectly reversible (Fig. 7).

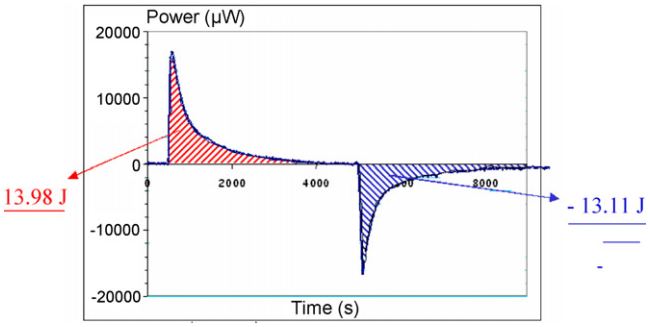

Fig. 7. Calorimetric signal during an oxygen adsorption/desorption cycle.

As previously mentioned, LSM is a non-stoichiometric compound. At high temperature and pressure LSM is over-stoichiometric in oxygen due to the formation of cation vacancies [25], leading to significant oxygen transfers between gas and solid phases. Indeed, thermogravimetric tests (not presented here [2]) have shown that the mass increase due to oxygen transfer for nonstoichiometric reasons (Δm_{stoi}) is predominant compared to that resulting from adsorption (Δm_{ads}). Therefore, it is necessary to distinguish the heat released by adsorption (Q_{ads}) from the heat released due to the equilibrium between oxygen and LSM (Q_{stoe}). The following equations express the mass and heat balance during the adsorption experiment, respectively, Δm_{exp} and Q_{exp}:

$$\Delta m_{\text{exp}} = \Delta m_{\text{ads}} + \Delta m_{\text{stoi}} \tag{2}$$

$$Q_{\text{exp}} = Q_{\text{ads}} + Q_{\text{stoi}} \tag{3}$$

The measured total area under the power signal, Q_{exp}, can be expressed as a function of the enthalpies of adsorption and reaction as follows:

$$\frac{Q_{\text{exp}}}{m} = S_{\text{BET}} \sum_{i=1}^{n} \Gamma_i \theta_i \Delta H^{\circ}_{i\,\text{ads}} + \frac{\delta \Delta H^{\circ}_{\text{stoi}}}{M_{\text{LSM}}} \tag{4}$$

where M_{LSM} is the LSM molar mass, S_{BET} the specific surface area of the sample and m its mass, δ the LSM oxygen non-stoichiometry ($La_{0.8}Sr_{0.2}MnO_{3+\delta}$), $\Delta H^{\circ}_{\text{stoi}}$ the reaction enthalpy between LSM and O_2, and $\Delta H^{\circ}_{i\,\text{ads}}$ the adsorption enthalpy of the ith oxygen adsorbed species, Γ_i and θ_i are respectively the amount of adsorption sites i by unit of area and the corresponding surface coverage ($0 < \theta_i < 1$).

From the study of the experimental values obtained by Kuo et al. [23] and as detailed in Appendix A, $\Delta H^{\circ}_{\text{stoi}}$ is equal to −25 kJ/mol, and values for δ can be obtained according to pressure/temperature conditions. It is therefore possible to determine the value of the heat dispersed by the insertion reaction, and to get the term related to the enthalpies of adsorption for each experiment.

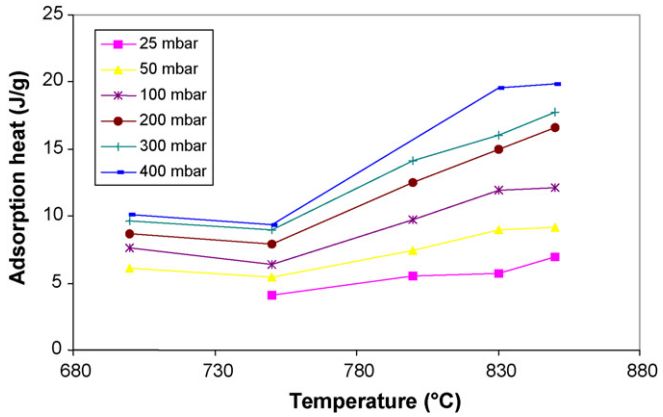

Fig. 8. Heat released due to adsorption of oxygen as a function of temperature for different oxygen pressures.

The graph of the heat of adsorption, $S_{\mathrm{BET}} \sum_{i=1}^{n} \Gamma_i \theta_i \Delta H^{\circ}_{i\,\mathrm{ads}}$ as a function of temperature is shown in Fig. 8. It reveals that a change in behaviour of the total oxygen chemisorption heat occurs above 800 °C. This result implies that at this temperature the presence of oxygen at the surface of LSM particles is modified (either in numbers or in nature). This result confirms previous conclusions deduced from DRIFTS and TPD experiments.

All of this is of great interest when considered in conjunction with the difficulties in finding a single mechanism and a single rate-limiting step in the whole range of temperature of operation of the LSM cathodes in SOFC. In particular, we have done a detailed study of the kinetics of oxygen reduction at LSM cathodes by impedance spectroscopy and the interpretation of our results [2] (that will be published elsewhere [22]) lead us to consider different mechanisms (due to different oxygen chemisorbed species) above and under 800 °C.

4. Conclusion

This study, devoted to a better understanding of the surface properties of LSM in relation with its use as a cathode in SOFC devices, using complementary techniques, and combining different post-treatments of the samples, has enlighten on various aspects:

- from XPS the segregation of Sr has been evidenced according to post-treatments conditions: at very high temperatures ~1200 °C, or at lower temperatures and either in oxygen poor atmosphere or under cathodic polarisation;
- from TPD, several distinct oxygen species at the surface of LSM have been identified from which at least two species that desorb at temperatures higher than 800 °C;
- from DRIFTS, it has been possible to identify at 600 °C at least two species, attributed to O_2^- and O_2^{2-};
- from calorimetry, a change in the heat released by the adsorption of oxygen on LSM was observed at a temperature higher than 800 °C, signifying a change in the oxygen chemisorbed species nature and/or amount.

All these conclusions are of interest for the characterisation of LSM surface properties and can help to elaborate a mechanism capable of interpreting the kinetics of the processes observed at SOFC cathodes. The variety of effects caused by a change in temperature, oxygen pressure or polarisation, is sufficient to explain the disparities found in the literature concerning mechanisms and rate-limiting steps of the oxygen reduction reaction occurring at LSM cathodes.

Acknowledgements

We are grateful to P. Passet from Centre SMS at the Ecole Nationale Supérieure des Mines de Saint Etienne for conducting the XPS analysis and to the GDR (research group ITSOFC-700) of the CNRS for fruitful discussions.

Appendix A

A.1. LSM oxygen non-stoichiometry

The structure elements in the non-stoichiometric $La_{0.8}Sr_{0.2}MnO_{3+\delta}$ compound (in the oxygen excess region) are in Kroger–Vink notation: La_{La}^{x}, Sr_{La}', V_{La}''', Mn_{Mn}^{x}, Mn_{Mn}°, V_{Mn}''', O_{o}^{x}.

Equilibrium between LSM and oxygen can be written as follows

$$Mn_{Mn}{}^{x} + \tfrac{1}{4}O_2 = \tfrac{1}{6}V_{La}''' + \tfrac{1}{6}V_{Mn}''' + Mn_{Mn}\circ + \tfrac{1}{2}O_O{}^{x} \quad (A.1)$$

The equilibrium constant is

$$K = \frac{[V_{La}''']^{1/6}[V_{Mn}''']^{1/6}[Mn_{Mn}\circ]}{P_{O_2}^{1/4}[Mn_{Mn}^{x}]} \quad (A.2)$$

According to the work published by Kuo et al. [23], the assumption is made that

$$[V_{La}'''] = [V_{Mn}'''] = \frac{\delta}{3} \quad (A.3)$$

The electroneutrality equation is

$$[Mn_{Mn}\circ] = 3[V_{La}'''] + 3[V_{Mn}'''] + [Sr_{La}'] = 6[V_{La}'''] + [Sr_{La}'] = 2\delta + x \quad (A.4)$$

The conservation of 'Mn' sites is expressed by

$$[Mn_{Mn}{}^{x}] + [Mn_{Mn}\circ] + [V_{Mn}'''] = 1 \quad (A.5)$$

which leads to

$$[Mn_{Mn}{}^{x}] = 1 - (x + 2\delta) - \frac{\delta}{3} = 1 - x - \frac{7\delta}{3} \quad (A.6)$$

The constant K is then written as follows (which is different from Kuo's):

$$K = \frac{[V_{La}''']^{1/3}[Mn_{Mn}\circ]}{P_{O_2}^{1/4}[Mn_{Mn}{}^{x}]} = \frac{(\delta/3)^{1/3}(2\delta + x)}{P_{O_2}^{1/4}(1 - x - 7\delta/3)} \quad (A\text{-}7)$$

Table A.1
Values of δ (the oxygen non-stoichiometry for $La_{0.8}Sr_{0.2}MnO_{3+\delta}$), K (the O_2/LSM equilibrium constant), and the related enthalpy and entropy

x	Pressure	Temperature (K)	δ [23]	K	ΔH° (kJ/mol)	ΔS° (J/mol)
0.2	1 atm	1273	0.050	1.12×10^{-1}	−25	−38
		1373	0.035	8.52×10^{-2}		
		1473	0.033	8.18×10^{-2}		

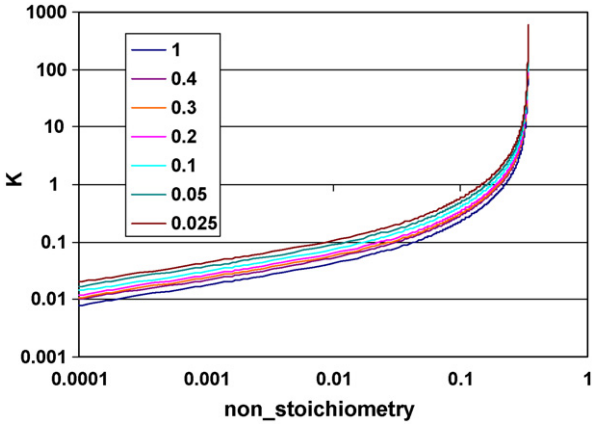

Fig. A.1. Abacus relating the value of K, the O_2/LSM equilibrium constant reaction to the oxygen non-stoichiometry δ for $La_{0.8}Sr_{0.2}MnO_{3+\delta}$, depending on the pressure (atm).

From the experimental values of δ obtained by Kuo at different oxygen partial pressures, it is possible to get the value of K at the different temperatures tested and thereby to reach the corresponding reaction enthalpy and entropy (cf. Table A.1).

It is then possible to create an abacus of K as a function of δ for different pressures (see Fig. A.1) so as to get, for given pressure and temperature conditions (those of our experimental conditions), the expected value of δ.

NB: These values obtained by this way are over-estimated at high pressure, low temperature (∼700 °C). Mizusaki et al. [26] have shown that a maximum value of +0.07 exists for δ.

References

[1] N.Q. Minh, J. Am. Ceram. Soc. 76 (1993) 563.
[2] N. Caillol, PhD, Saint-Etienne, France, 2006.
[3] H. Kamata, A. Hosaka, J. Mizusaki, H. Tagawa, Solid State Ionics 106 (1998) 237.
[4] E. Siebert, A. Hammouche, M. Kleitz, Electrochim. Acta 40 (1995) 1741.
[5] J. van Herle, A.J. Mc Evoy, K. Ravindranathan Thampi, Electrochim. Acta 41 (1996) 1447.
[6] E.P. Murray, T. Tsai, S.A. Barnett, Solid State Ionics 110 (1998) 235.
[7] Y. Takeda, R. Kanno, M. Noda, Y. Tomida, O. Yamamoto, J. Electrochem. Soc. 134 (1987) 2656.
[8] M. Østergård, M. Mogensen, Electrochim. Acta 38 (1993) 2015.
[9] J. Mizusaki, H. Tagawa, K. Tsuneyoshi, A. Sawata, J. Electrochem. Soc. 138 (1991) 1867.
[10] M. Gödickemeier, K. Sasaki, L.J. Gauckler, I. Riess, Solid State Ionics 86–88 (1996) 691.
[11] F.H. van Heuveln, H.J.M. Bouwmeester, J. Electrochem. Soc. 144 (1997) 126.
[12] G.E. Youngblood, A.S. Rupaal, L.R. Perderson, J.L. Bates, in: Proceedings of the Third International Symposium on SOFCs, Honolulu, October 17–22, (1993), p. 585.
[13] M. Kuznzcov, P. Otschik, P. Obenaus, K. Eichler, W. Schaffrath, Solid State Ionics 157 (2003) 371.
[14] J. Mizusaki, T. Saito, H. Tagawa, J. Electrochem. Soc. 143 (1996) 3065.
[15] M. Mogensen, K. Vels Jensen, M. Juhl Jorgensen, S. Primdahl, Solid State Ionics 150 (2002) 123.
[16] J.H. Scofield, J. Electron Spectr. Related Phen. 8 (1976) 129.
[17] S.P. Jiang, J.G. Love, J.P. Zhang, M. Hoang, Y. Ramprakash, A.E. Hughes, S.P.S. Badwal, Solid State Ionics 121 (1999) 1.
[18] S.P. Jiang, J.G. Love, Solid State Ionics 138 (2001) 183.
[19] S. Ponce, M.A. Peña, J.L.G. Fierro, Appl. Catal. B: Environ. 24 (2000) 193.
[20] Q.-H. Wu, M. Liu, W. Jaegermann, Mater. Lett. 59 (2005) 1480.
[21] L.C. Dufour, G.L. Bertrand, G. Caboche, P. Decrose, A. El Anssari, A. Poirson, M. Vareille, Solid State Ionics 101–103 (1997) 661.
[22] N. Caillol, M. Pijolat, E. Siebert, in press.
[23] J.H. Kuo, H.U. Anderson, D.M. Sparling, J. Solid State Chem. 83 (1989) 52.
[24] M. Che, A.J. Tench, in: D.D. Eley, H. Pines, P.B. Weisz (Eds.), Advances in Catalysis, vol. 32, Academic Press, New York, 1983.
[25] S. Miyoshi, J.-O. Hong, K. Yashiro, A. Kaimai, Y. Nigara, K. Kawamura, T. Kawada, J. Mizusaki, Solid State Ionics 154/155 (2002) 257.
[26] J. Mizusaki, N. Mori, H. Takai, Y. Yonemura, H. Minamiue, H. Tagawa, M. Dokiya, H. Inaba, K. Naraya, T. Sasamoto, T. Hashimoto, Solid State Ionics 129 (2000) 163.